

Constraining Dark Energy with the DEEP2 Redshift Survey

Marc Davis^{1,2}, Brian F. Gerke², and Jeffrey A. Newman³
for the DEEP2 Team

¹ *Department of Astronomy, University of California—Berkeley, USA*

² *Department of Physics, University of California—Berkeley, USA*

³ *Lawrence Berkeley National Laboratory, USA*

Abstract.

The DEEP2 survey has now completed half of its planned three-year lifespan, and we have collected approximately 50% of the data, putting us exactly on schedule. The survey plan calls for spectroscopic coverage by July of 2005 of $\sim 60,000$ galaxies over 3.5 square degrees to a limiting magnitude of $R_{AB} = 24.1$; the great majority of these objects are at $0.7 < z < 1.4$. We describe here one method by which DEEP2 can set constraints on the equation of state parameter of the Dark Energy, w . By counting the number of virialized groups and clusters we find in redshift space as a function of their redshift and internal velocity dispersion, we probe both the volume element and the growth of structure at $z \sim 1$, each of which depends on w . Studies of early DEEP2 data indicate that the method is likely to work, and preliminary indications are that a total of ~ 250 small groups will be counted in the full survey, leading to a constraint $\delta w \sim 0.1$ if combined with both the velocity dispersion distribution of $z \sim 0$ clusters from the Sloan Digital Sky Survey and an independent measurement of σ_8 . We also provide a general description of the DEEP2 observations and target selection, including the algorithm by which galaxies are placed on slitmasks, to provide context for discussion of DEEP2 cluster samples.

1. Introduction

The DEEP2 (Deep Extragalactic Evolutionary Probe 2) survey is being led by a consortium of astronomers at the University of California at Berkeley and the University of California at Santa Cruz who are pooling their Keck telescope time to gather spectra of $\sim 60,000$ galaxies, most of which fall in the redshift range $0.7 < z < 1.4$. As of this writing, we are pleased to announce that the survey is halfway complete, and the list of scientific investigations currently underway is longer than the list of collaborators (~ 2 dozen). In this proceeding, we provide an update on prospects for constraining the Dark Energy equation of state parameter, w , by counting groups of galaxies in DEEP2 as a function of their redshift and velocity dispersion. DEEP2 was designed to study galaxies over several, independent, comparatively wide fields; this will provide large enough samples and small enough cosmic variance to measure w using large-scale structure in the DEEP2 fields.

We will begin our discussion by briefly summarizing the observational program of the DEEP2 survey. The survey will be described in more detail in an

upcoming paper by Faber et al. (2004). We then discuss the theoretical basis for measuring w using counts of galaxy groups. To provide a preview of the measurement we will make with the final DEEP2 catalog, we identify and count groups in the current DEEP2 data and compare these measurements to expectations from realistic DEEP2 mock catalogs produced from N-body simulations. We finish by computing the cosmological constraints that are expected from such a measurement.

2. Details of the Observations

The University of California has guaranteed DEEP2 80 nights of dark observing time at the Keck Observatory over 3 years. The survey is made possible by DEIMOS, a new multi-object spectrograph on the Keck 2 telescope (Faber et al. 2002). DEIMOS' large field of view ($16' \times 5'$), large detector mosaic ($8k \times 8k$ pixels, allowing broad spectral coverage at high resolution), and active-feedback Flexure Compensation System (which allows the effects of fringing to be removed, greatly improving sky subtraction) are all key to our survey strategy and its success. DEIMOS was commissioned in June 2002, and the DEEP2 survey began immediately thereafter, in July. This review is written after 3 semesters of observing, out of a total of 6; current plans call for observing to be completed in July, 2005. At the halfway point, we have observed 245 of 480 DEIMOS slitmasks, and collected spectra for $\sim 30,000$ galaxies. Needless to say, our small team is barely keeping up with the huge influx of data!

2.1. The DEEP2 Fields

The Survey is designed to observe during the months of April through October at the Keck observatory on Mauna Kea, Hawaii. There are 4 fields spaced by ~ 60 degrees, allowing us always to move from one field to the next while the fields are at small zenith angle. The 3.5 square degrees of field coverage is divided amongst our four fields spread across the sky as shown in Table 1. For the first field, we target galaxies with $R_{AB} < 24.1$ in an $120'$ by $16'$ region of sky. The long axis of this field, known as the Extended Groth Strip (EGS), is oriented along a line of ecliptic latitude, allowing extremely efficient mid-IR imaging with the *Spitzer Space Telescope*. It is the subject of some of the deepest wide-area ($120' \times 10'$, embedded within the region observed by DEEP2) *Spitzer* imaging on the sky, currently being conducted by the MIPS and IRAC instrument teams (Fazio et al., 2004; Papovich et al., 2004). This field is also the focus of a large *Hubble Space Telescope* Advanced Camera for Surveys campaign now underway, covering a $60' \times 10'$ region in the middle of the *Spitzer* coverage in both V and I , along with deep *GALEX*, *Chandra*, and *XMM* imaging.

The remaining fields of DEEP2 use deep BRI imaging obtained with the CFH12K camera on the Canada France Hawaii Telescope (Coil et al. 2004) to pre-select galaxies with $z > 0.7$ by means of a simple color cut (Newman et al. 2004). This pre-selection allows us to observe galaxies at high redshift efficiently; based on studies using data from the Extended Groth Strip (where no color cut is applied), more than 60% of galaxies with $R_{AB} < 24.1$ are at $z < 0.75$, but only 13% of galaxies that pass the color cut are; while only 3% of objects rejected are at $z > 0.75$. Each of these fields comprises three imaging

Field Number	RA	δ	area (deg ²)	fraction observed
1	14 ^h 17 ^m	+52 30	0.5	0.25
2	16 ^h 52 ^m	+34 55	1.0	0.35
3	23 ^h 30 ^m	+0	1.0	0.70
4	2 ^h 30 ^m	+0	1.0	0.50

Table 1. Summary of the DEEP2 fields. Shown are the locations, areas on the sky, and currently observed fraction for each of our four fields.

pointings of CFHT, covering a total area of 120' by 30' and oriented with the long direction East-West.

2.2. The DEEP2 Sample

There are approximately 10^5 galaxies with $R_{AB} < 24.1$ and $z > 0.7$ in the 3.5 sq. degrees surveyed; because of slitmask design constraints and the finite amount of observing time available, we are able to obtain spectra for only $\sim 60,000$ of these potential targets. Of the observed galaxies, we will successfully obtain redshifts for $\sim 50,000$, and resolved kinematics (e.g. rotation curves) for $\gtrsim 5000$. Based on follow-up studies, it appears that the majority of DEEP2 redshift failures are objects at $z > 1.4$, which lack features in our spectroscopic window (Steidel, private communication 2003). Crudely, one can think of the DEEP2 sample as having twice the number of objects and 3 times the volume as the Los Campanas Redshift Survey (Shectman et al. 1996), but at $z \sim 1$ rather than $z \sim 0$. The total volume to be surveyed ($\sim 6 \times 10^6 h^{-3} \text{Mpc}^3$ comoving, assuming a standard Λ CDM cosmology) should not contain many extremely rich clusters, but is sufficient for counting less extreme objects like galaxies and groups of galaxies. Having four independent fields both limits the impact of and allows us to measure the effects of cosmic variance.

In studying surveys which cover a broad redshift range such as DEEP2, it is important to understand that such a sample will inevitably select different sorts of galaxies at different redshifts. For instance, the R band in which the DEEP2 sample is magnitude-limited corresponds to restframe $\sim 4000\text{\AA}$ at $z \sim 0.7$, but to $\sim 2800\text{\AA}$ at $z \sim 1.4$. Thus our wide redshift range means that galaxies are not selected based on the same rest-frame properties at different redshifts; one must be mindful of how homogeneous any sample of galaxies covering a broad redshift range actually is.

For instance, galaxies with “early-type” spectra (i.e., spectra which resemble those of low-redshift elliptical and S0 galaxies) are redder than late-type galaxies that are forming stars; so for a given rest-frame B or R absolute magnitude and redshift, an early-type galaxy will be fainter than a late-type galaxy in the observed R band. This effect becomes stronger as one moves to higher redshift and the rest-frame band corresponding to observed R becomes bluer. It is important to note that this effect cannot be removed simply by selecting objects in redder wavebands. Even surveys which target galaxies for spectroscopy based on infrared magnitudes (e.g. K) are likely not to measure redshifts for objects

that are faint in the optical, so they too will tend to lose intrinsically red objects from their sample before bluer ones due to redshift failures, while simultaneously only the brightest intrinsically blue objects will fulfill the sample's selection criteria. As a practical matter, for DEEP2 samples these effects mean that our sample probes deeper into the luminosity function for blue galaxies (compared to the L_* for blue galaxies) than it does for red galaxies (compared to the L_* for red galaxies; for $z \gtrsim 1.1$, early-type galaxies are all but absent from the DEEP2 sample).

Although we define which galaxies we wish to observe by means of the magnitude limit and color cut, it is impossible to place all of them on DEIMOS slitmasks for observation. No two slitlets can have overlapping spectra (as otherwise the skylines from one hopelessly contaminate the other), and it is all but impossible to achieve effective sky subtraction for slits less than 3 arcsec long; these two requirements limit the number of slitlets we can place on a mask. These constraints imply that two objects separated by less than ~ 3 arcsec in the direction parallel to the long axis of a mask cannot both be observed simultaneously, regardless of their location in the short ($4'$) direction.

To mitigate this effect, nearly every position on the sky in the DEEP2 survey is covered by at least 2 masks, giving objects multiple opportunities to be selected. We also assign each object a weight W between 0 and 1 according to its probability of being a galaxy as opposed to a star (cf. Coil et al. 2004), its R magnitude (if fainter objects are not deweighted somewhat, the sample will tend to pile up at the magnitude limit of the survey), and its consistency with the color cut (outside the nominal cut, the W falls off as a Gaussian with $\sigma = 0.05$; this provides a 'prewhitening' of the color selection at a level greater than our estimated systematics in $B - R/R - I$ space). This weight is used for randomly selecting amongst objects that would have overlapping spectra, as discussed below, allowing us to focus on objects with the desired characteristics while still sampling a wider parameter space.

For fields other than the Extended Groth Strip, objects are allocated among these multiple slitmasks through a two-stage procedure (in the EGS, each point on the sky is covered by 4 masks with two different orientations; we thus use a somewhat more complicated algorithm than that described here, though it is largely analogous). The first stage, or 'pass', places slitlets only in a central region unique to each mask – 2 arcmin wide on average, though this varies somewhat due to the adaptive tiling of masks (q.v. below). This central region is favored because galaxies at one end of the mask or the other in the short axis will have different wavelength coverage on the detector (as this axis corresponds to the spectral direction in DEIMOS). The wavelength shift is $\sim 100 \text{ \AA}/\text{arcmin}$, so that this is not a very strong effect, but nonetheless one of which we are mindful. The central target selection region for each slitmask is not actually rectangular on the sky, but instead is bowed parallel to a line of constant central wavelength on the DEIMOS detector (which is not straight on the sky due to optical distortions).

In the first pass, we initially trim the list of targets by generating a random number between 0 and 1 and only retaining those for which the random number is less than their weight, so low- W objects (e.g. those which are likely to be stars) are only rarely placed on slits in the central portion of a mask. We then

search this trimmed list for cases where we can place two objects (separated by less than 3 arcsec in the long direction of the mask) on a single slit which has PA relative to the mask of less than 30° . Slits are allocated to all such cases, boosting our ability to study close pairs of galaxies. We then generate a random priority, P_1 , for each of the remaining objects in the trimmed list. Each one that can be observed without precluding any other is always selected for observation, while in cases of conflict the object with greatest P_1 is taken. This procedure (initial selection according to W , random selection amongst the surviving targets) yields a sample where the probability of selection is directly proportional to an object's weight, making the best possible use of the central region of each mask.

In the second pass, objects are selected over the full $16' \times 4'$ area covered by the mask, rather than just the central region. Objects are given a priority in the second pass, P_2 , equal to their weight, W , divided by a random number between 0 and 1. We then assign slits to objects in decreasing order of P_2 , until every object either has been selected or conflicts with a slit on that mask. Since any target object that can be placed on a mask without causing a conflict is put on that mask, in the second pass low- W objects will often be selected for observation, since doing so is cost-free. The second pass proceeds from west to east amongst the masks, in order.

The second pass again ranks galaxies in priority using their weights and random numbers, but now over the full $16' \times 4'$ area covered by the mask, rather than just the central region. Slits are then allocated to galaxies in descending order of priority, so long as they do not conflict with any slit that has already been added to the mask. In the end, any target object that can be placed on a mask without causing a conflict is put on that mask, so that in the second pass low-weight objects will frequently be selected for observation, since they are cost-free. The second pass proceeds from west to east amongst the masks, in order.

Cosmic variance in the number of targets within a $16' \times 2'$ region is high; if masks are evenly spaced, some will have many fewer slits than others. To avoid this, we iteratively adjust the positions (and, correspondingly, the widths of the central region) of each mask such that the number of targets selected in the first pass is constant mask-to-mask. This enables us to obtain spectra for a uniform fraction of galaxies over the survey region.

In the end, we select $> 60\%$ of the eligible galaxies for spectroscopy. In using such a sample to study large-scale structure, it is important to realize that the selection of targets for spectroscopy causes the two-point autocorrelation function $\xi(r)$ to be distorted (Coil, Davis, & Szapudi 2001). These authors show that the effect on the measured $\xi(r_p, \pi)$ is modest, with the principal impact being a reduction in the elongation of contours of ξ at small separation due to 'fingers of god', corresponding to a reduction in velocity dispersion by $\sim 20\%$. Figure 1 shows actual mask designs for a portion of one DEEP2 field.

At the end of this process, each slitmask contains ~ 110 -150 slitlets, typically ~ 7 arcsec long but spanning the range $\sim 3 - 15+$ arcsec, over a $16'$ by $4'$ region. The long axis of an individual slitlet is oriented along the major axis of each galaxy measured from the CFHT photometry, so long as that axis is within ± 30 degrees of the long axis of the slitmask and the galaxy is measurably ellipsoidal.

Each mask is observed for at least 3 20-minute exposures with the 1200 l/mm grating on DEIMOS, centered at 7800 Å. This setting provides comparatively high-resolution ($R \gtrsim 5000$) spectroscopy over a 2600 Å window. Observing at high resolution has two major advantages: it allows us to split the [OII] 3727 Å doublet feature, providing a secure redshift for line-emitting objects at $0.7 < z < 1.4$ even if that is the only feature available; and it effectively provides OH suppression, since only $\sim 20\%$ of all pixels are influenced by skylines in this setting, yielding large domains of skyline-free spectrum (our sky subtraction is effective on the skylines as well; if we compare the redshift distribution of DEEP2 sources to the sky spectrum, matching wavelength to redshift by assuming that the z was measured from [OII], we find a correlation coefficient of only -0.1) Under optimal conditions, we can observe 8 masks per night, which will yield spectra of ~ 1000 -1200 galaxies.

3. Using the DEEP2 Survey to Study Dark Energy

DEEP2 can set constraints on the dark energy through two variants on a classical cosmological test, the 'dN/dz test'. This test can constrain cosmological parameters like the mass and dark energy density parameters Ω_m and Ω_X , or the dark energy equation of state parameter w , by measuring the apparent abundance per unit redshift and solid angle, dN/dz , of a class of objects. The abundance depends on fundamental cosmological parameters and comoving number density via the relation

$$dN/dz = n(z)dV/dz \propto n(z)r(z)^2/E(z)dz, \quad (1)$$

where z is the redshift of interest; $n(z)$ is the comoving number density of this class of object at that redshift; dV/dz is the amount of comoving volume per unit redshift and solid angle; $E(z)$ is the familiar Hubble ratio, given by

$$E(z) \equiv H(z)/H_0 = (\Omega_m(1+z)^3 + \Omega_X(1+z)^{3(1+w)})^{1/2} \quad (2)$$

at late times (and assuming that w is independent of z); and $r(z)$ is the comoving distance to redshift z ,

$$r(z) = (c/H_0) \int dz/E(z). \quad (3)$$

The relationship between number counts and cosmology formed the basis of some of the earliest attempts to determine the geometry of the Universe (Hubble 1926).

In general, this test has been applied in one of two limits: where $n(z)$ is presumed to be known (e.g. Loh & Spillar 1986), or where $n(z)$ is much more sensitive to cosmology than the volume element dV/dz (e.g. studies of X-ray cluster abundances, [Borgani et al. 2004; Bahcall et al. 1997]). The DEEP2 Redshift Survey has the potential to provide cosmological constraints spanning both of these limits. Newman & Davis (2000) showed that the comoving abundance of dark matter halos with circular velocity ~ 200 km/sec – those which presumably host typical L_* galaxies – normalized to the abundance observed at $z \sim 0$ is almost entirely independent of cosmological parameters. However,

the application of this method is limited by our ability to predict the general effects of baryonic infall (Newman & Davis 2002) and the lack of a matching sample at $z \sim 0$ for normalization (local, fiber-based surveys such as SDSS only measure the linewidth of gas at the centers of galaxies, which may not reflect the kinematics of the dark matter halo); we therefore are concentrating on other methods in the short term.

In contrast to typical galaxies, $n(M, z)$, the comoving abundance of rich galaxy clusters as a function of their mass, M , and redshift, z , is exponentially sensitive to the growth rate of large-scale structure, which depends on cosmological parameters including w (Linder & Jenkins, 2003). Exploiting this fact, the dN/dz test has been applied by using X-ray properties or optical richnesses of clusters, and should be possible with other methods (e.g. blind Sunyaev-Zel'dovich effect surveys) in the future.

Apart from the difficulty of finding them in X-ray or optical photometric surveys, there is no fundamental reason why poorer groups cannot be incorporated into such analyses; because their comoving abundance is less sensitive to structure formation than more massive objects, they provide constraints in different directions in the $\Omega_m - w$ plane than more massive clusters, so a simultaneous analysis will yield more information than a study of rich clusters alone. However, the only currently effective method for finding less massive groups with few luminous members is to detect them in redshift space, as their X-ray brightness is low (especially at higher redshift) and their contrast against background galaxies in surface density is poor.

As a free byproduct, the group line-of-sight velocity dispersion, σ , which roughly obeys the relation $\sigma \propto M^{1/3}$, is determined in the process of finding groups in redshift space. The velocity dispersion distribution of dark matter halos can be predicted either from analytic methods like Press-Schechter or N-body simulations, much like the mass distribution; in hydrodynamic simulations, it is much more strongly correlated with cluster mass than gas diagnostics like X-ray temperature (Evrard 2004). Understanding the details of the relationship between what is measured and the true halo velocity dispersion still poses some challenges—*e.g.*, the nature and extent of galaxy “velocity bias” remains uncertain. However, these topics are the subject of a variety of simulation efforts, and we have every expectation that a resolution should be reached in the next few years; observational results will stand unchanged, but their interpretation could improve over time.

As suggested by Newman et al. (2002), the DEEP2 Redshift Survey is now providing data on groups to $z \sim 1.4$ that can be used for this test. We have implemented a sophisticated cluster-finding algorithm (Marinoni et al. 2002, Gerke et al. 2004) which finds groups adaptively using the locations of galaxies in redshift space. This removes most of the background contamination problems of photometric methods, but not all (since galaxies cluster with each other and velocity dispersions can correspond to ~ 20 Mpc in length, interloper contamination is inevitable). Furthermore, as described in §2.2, we cannot get spectroscopy for every object, especially in the densest regions; *e.g.*, sometimes we will lose 2 members out of a 3-member group by chance, causing the group not to be identified. However, extensive tests with mock catalogs (Yan et al. 2004) have shown that we recover the *velocity distribution* of clusters for $\sigma > 400$ km/sec

to well within the expected cosmic variance in group counts, and that we find groups equally effectively across the DEEP2 redshift range and over a wide span in velocity dispersion, yielding a nearly unbiased sample.

Some results from our search for galaxy groups can be seen in Figure 2, which shows the measured group velocity distribution from 1/12th of the total planned DEEP2 dataset. Random errors for the full DEEP2 sample will be only $\sim 1/3$ as large. Also plotted are the average actual $n(\sigma)$ distribution for groups in twelve mock DEEP2 samples from Yan et al. (2004); and the RMS variation of those mocks about that line, due to Poisson statistics and cosmic variance (shaded region). As can be seen in Figure 3, the typical group found in DEEP2 has only a few members luminous enough to be targeted for spectroscopy ($\sim L_*$ or brighter at $z \sim 1$), so the contrast between these groups and the field is extremely poor when there is no redshift information available.

Some examples of the difficulties in identifying poor groups and their members are shown in Figure 4, which depicts two real groups and two groups from a mock catalog plotted on the sky, as well as in redshift space. It is all but impossible to tell the difference; each real group has a doppelganger in the group catalog from simulations. The fingers of god are obvious and are much larger than our redshift precision, ~ 30 km/sec. The estimation of group velocity dispersion is clearly straight-forward; in the long term, we will be able to compare these to X-ray temperatures (many weak groups can be stacked to yield strong signal-to-noise), Sunyaev-Zel'dovich decrements, and lensing mass (at the low-redshift end), especially in the Extended Groth Strip where wide arrays of complementary data are available.

We expect to find ~ 250 groups and clusters in the full DEEP2 sample. As described by Newman et al. (2002), under the assumptions that σ_8 is known independently of cluster studies (e.g. by using galaxy-galaxy lensing to turn the clustering of galaxies into a clustering of mass, and hence σ_8), that the velocity dispersion distribution of groups at $z \sim 0$ has been measured by the Sloan Digital Sky Survey, and that the geometry of the Universe is flat, it is possible to constrain the dark energy equation of state parameter with a precision of $\delta w/w \sim 0.1$. We have recently started refining that analysis to prepare for applying these methods to the DEEP2 data; amongst other things, we find that the precision of this measurement is degraded only slightly when completely covariant systematic errors are incorporated into the analysis of Newman et al. We eagerly await the first results from this procedure, which we will tackle as soon as we finish observing and determining redshifts for DEEP2 galaxies, in mid-to-late 2005.

Acknowledgments. We thank our collaborators Sandy Faber, David Koo, and Puragra Guhathakurta and the hardworking teams at Berkeley and Santa Cruz. This project was supported by the NSF grant AST-0071048. BFG acknowledges support from an NSF Graduate Research Fellowship, and JAN acknowledges support by NASA through Hubble Fellowship grant HST-HF-01132.01 awarded by the Space Telescope Science Institute, which is operated by AURA Inc. under NASA contract NAS-5-26555.

References

- Bahcall, N., Fan, X. & Cen, R. 1997, *ApJ*, 485, 53.
Borgani, S. et al. 2004, *MNRAS*, 348, 1078.
Coil A. et al. 2004, in press.
Coil, Davis, & Szapudi 2001, *PASP*, 113, 1312.
Evrard, G. 2004, in “Clusters of Galaxies: Probes of Cosmological Structure and Galaxy Evolution from the Carnegie Observatories Centennial Symposia”, Cambridge University Press.
Faber et al. 2003, *SPIE*, 4841, 1657
Fazio, G. et al. 2004, astro-ph/0405595.
Gerke, B. F. et al. (2004), to be published
Hubble, E. 1926, *ApJ*, 64, 321.
Linder, E.V. & Jenkins, A. 2003, *MNRAS*, 346, 573.
Loh, E. D. & Spillar E. J. 1986, *ApJ*, 307L, 1L.
Marinoni C., Davis, M. Newman, J.A. & Coil, A. 2002, *ApJ*, 580, 122.
Newman, J.A. & Davis, M. 2000, *ApJ*, 534, 11.
Newman, J.A. et al. 2002, *PASP*, 114, 29.
Newman J.A., Marinoni, C., Coil, A. & Davis, M. 2002, *PASP*, 114, 29.
Papovich et al. 2004, astro-ph/0406035.
Shectman et al. 1996, *ApJ*, 471, 617.
Yan, R., White, M., Coil, A. 2004, *ApJ* 607, 739

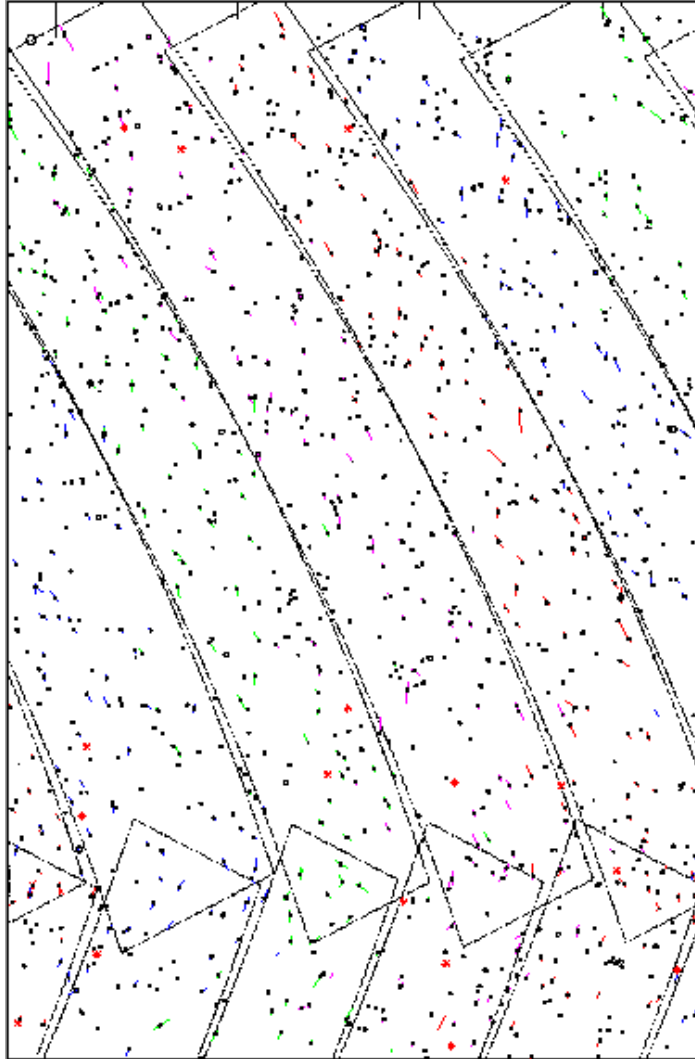


Figure 1. DEEP2 targets, slitlets, and masks in an $\sim 18' \times 10'$ region drawn from a $42' \times 28'$ CFHT pointing. Each pointing is tiled with two slightly-overlapping rows of masks, with the masks tilted to minimize the effects of atmospheric dispersion at the time of observation. Target selection for each row is done separately, allowing some objects to be observed twice for data quality testing. The dotted lines roughly indicate the central, “pass one” portion of each mask; ellipses show eligible DEEP2 targets. Each small rectangle plotted shows a DEEP2 slitlet to scale; its color indicates which mask the slit was placed on (note that most slits of the same color fall in the central portion of the mask corresponding to that color, but not all).

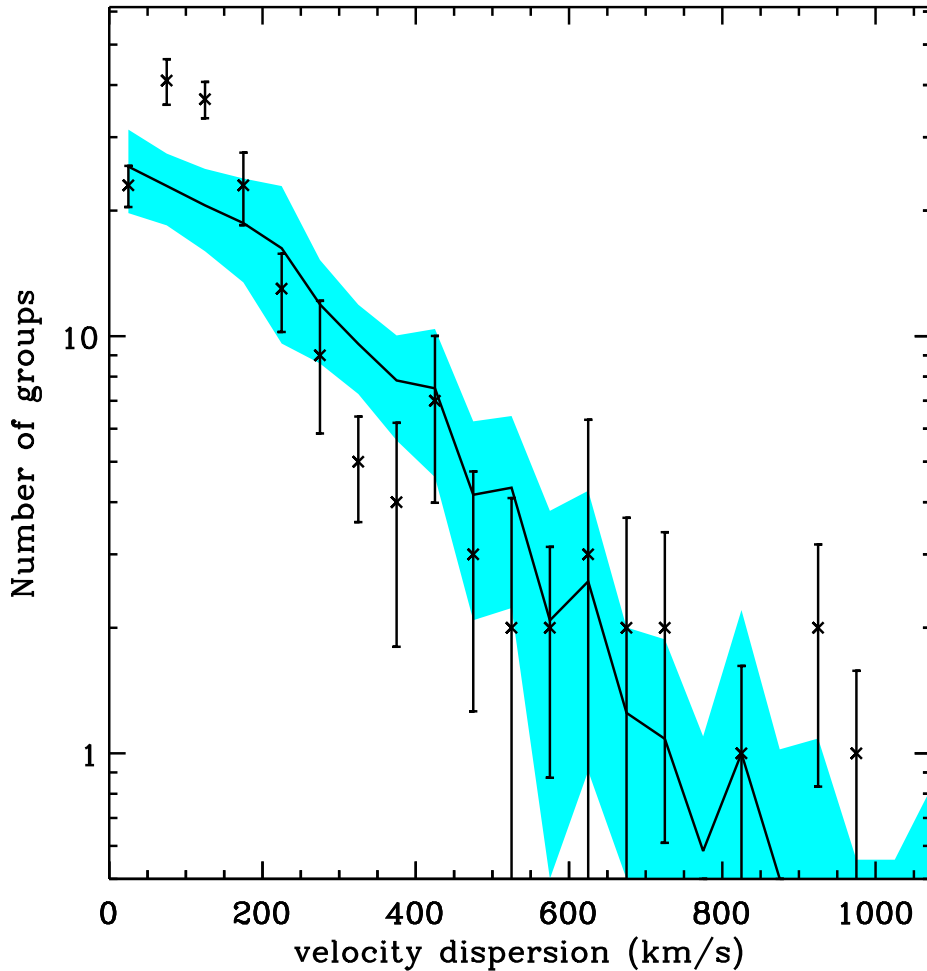


Figure 2. Comparison of the velocity function $n(\sigma)$ measured in a single DEEP2 pointing to that predicted by mock catalogs. The data points are the measured velocity function of groups found in the most uniformly observed DEEP2 pointing (Figures 3), in bins of 50 km/s. Error bars are estimated from applying the VDM group finder to twelve independent mock DEEP2 pointings, measuring $n(\sigma)$, and taking the standard deviation of the residuals $n_{\text{found}} - n_{\text{true}}$. The solid line is the average velocity function from the mock catalogs, $\langle n_{\text{true}}(\sigma) \rangle$, in bins of 50 km/s, and the shaded region indicates the cosmic variance (standard deviation) in each bin. The measured velocity function is consistent with the prediction in the regime ($\sigma > 400$ km/s) where an accurate measurement is expected based upon the mock catalogs.

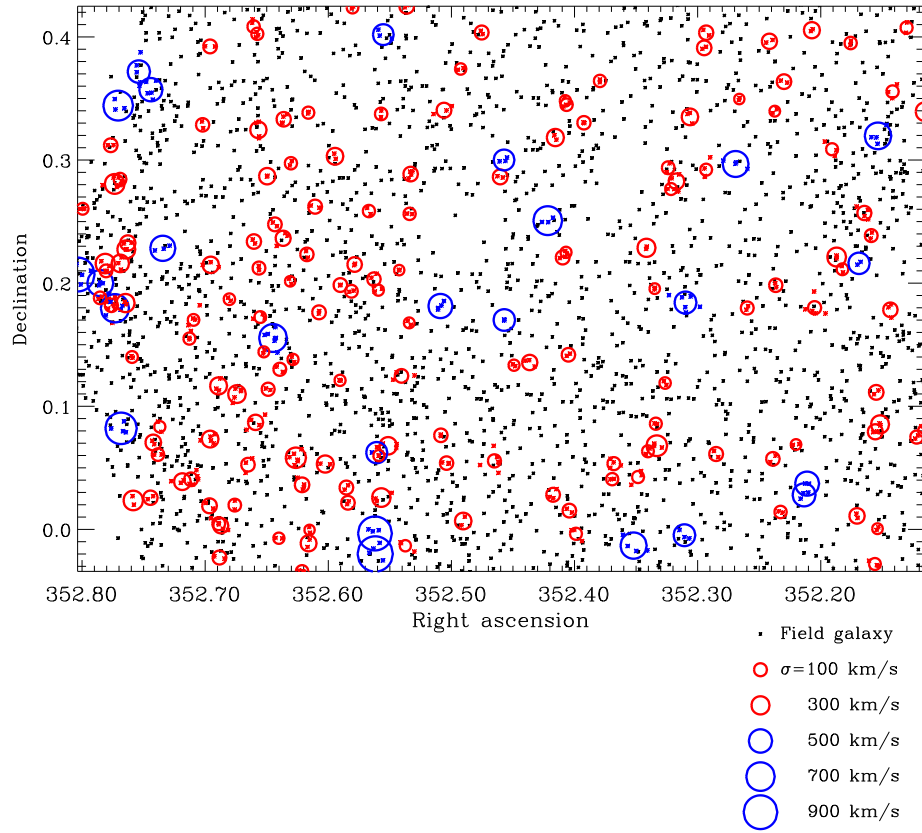


Figure 3. Groups in the most uniformly observed DEEP2 field, as seen on the sky. Colored circles indicate the position of the groups, with circle radius proportional to group velocity dispersion. Red circles denote groups with velocity dispersion $\sigma < 400$ km/s, and blue circles show $\sigma \geq 400$ km/s groups. Similarly, colored dots indicate group member galaxies. Isolated galaxies are shown by black dots.

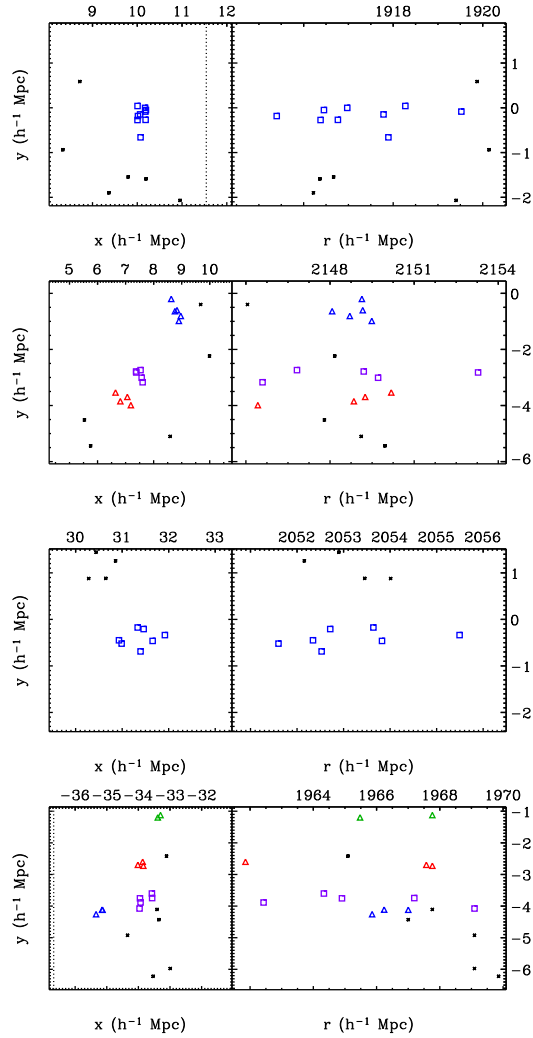


Figure 4. A selection of DEEP2 groups, shown as seen on the sky and projected in redshift space. Colored squares denote the galaxies in the group being shown; colored triangles show galaxies in nearby groups, and black points show nearby isolated galaxies. Dashed lines indicate the edge of the survey field. Two of the groups shown here come from real DEEP2 data, and two come from mock catalogs. Distinguishing between them is left as an exercise for the reader.